
**Separation Science and Technology**
Publication details, including instructions for authors and subscription information:
http://www.informaworld.com/smpp/title~content=t713708471

# Groundwater Cleanup by In-Situ Sparging. XIII. Random Air Channels for Sparging of Dissolved and Nonaqueous Phase Volatiles

David J. Wilson[a]; Ann N. Clarke[a]; Kathryn M. Kaminski[b]; Emmanuel Y. Chang[b]
[a] ECKENFELDER INC., NASHVILLE, TENNESSEE, USA [b] MARTIN LUTHER KING MAGNET HIGH SCHOOL, NASHVILLE, TENNESSEE, USA

**To cite this Article** Wilson, David J. , Clarke, Ann N. , Kaminski, Kathryn M. and Chang, Emmanuel Y.(1997) 'Groundwater Cleanup by In-Situ Sparging. XIII. Random Air Channels for Sparging of Dissolved and Nonaqueous Phase Volatiles', Separation Science and Technology, 32: 18, 2969 — 2992
**To link to this Article: DOI:** 10.1080/01496399708000790
**URL:** http://dx.doi.org/10.1080/01496399708000790

SEPARATION SCIENCE AND TECHNOLOGY, **32**(18), pp. 2969–2992, 1997

# Groundwater Cleanup by In-Situ Sparging. XIII. Random Air Channels for Sparging of Dissolved and Nonaqueous Phase Volatiles

DAVID J. WILSON and ANN N. CLARKE
ECKENFELDER INC.
227 FRENCH LANDING DR., NASHVILLE, TENNESSEE 37228, USA

KATHRYN M. KAMINSKI and EMMANUEL Y. CHANG
MARTIN LUTHER KING MAGNET HIGH SCHOOL
613 17TH AVE. N, NASHVILLE, TENNESSEE 37203, USA



## ABSTRACT

A mathematical model is developed to simulate the sparging of dissolved volatile organic compounds (VOCs) and nonaqueous phase liquid (NAPL) from contaminated aquifers. The sparging air moves through the aquifer in persistent, random channels, to which VOC must move by diffusion/dispersion to be removed. The dependence of the rate of remediation on the various model parameters is investigated and some practical conclusions are reached regarding the operation of air sparging wells for aquifer remediation. VOCs of low water solubility (such as alkanes) and present as NAPL are found to be removed by air sparging much more slowly than VOCs of higher water solubility (such as benzene, toluene, ethylbenzene and xylenes) and present as NAPL, due to the very small maximum concentration gradients which can be maintained around droplets of the former. These small concentration gradients result in very slow rates of NAPL solution.

## INTRODUCTION

The in-situ volatilization or biodegradation of volatile organic compounds (VOCs) in contaminated aquifers by air sparging has become established as one of the better technologies for dealing effectively and economically with groundwater contamination (1, 2). The American Academy

of Environmental Engineers has discussed sparging and biosparging extensively in two of its recent books on innovative technologies for site remediation (3, 4), and both the 1993 and 1995 Bioreclamation Symposia devoted extensive coverage to these topics (5, 6).

Several papers in this last reference (6) raised some serious questions about the nature of air and water movement in the vicinity of an air injection well (7–11), which markedly affects the rate of mass transport of VOCs from the aquifer to the sparging air and, in the case of biosparging, the transport of oxygen from the sparging air to the aquifer aqueous phase. The points of particular significance are the following. First, the steady injection of air into an aquifer via the standard sparging well produces virtually no bulk circulation of water in the vicinity of the well. Second, the injected air moves up to the top of the aquifer not as isolated, independent, random bubbles, but in persistent channels. There is common agreement that these facts bode ill for the efficiency of mass transport between the gas and aqueous phases in sparging. Pulsed operation of the air injection well has been proposed as a means to increase the dispersivity, and thereby the rate of mass transport, in sparging.

We have mathematically modeled sparging with air channeling for dissolved VOCs (12), nonaqueous phase liquid (NAPL, 13), and biosparging of NAPL and dissolved VOC (14), and have developed a formula for estimating the effect of pulsed operation on the dispersivity.

We note that these problems do not arise in sparging operations in which vacuum-vaporizer-wells (15, 16) or aeration curtains (17) are used.

Our earlier sparging models (12–14) included channeling in a quite homogeneous and rather artificial way. A well-behaved mathematical function was postulated for the vertical molar flux of the injected gas, the horizontal flux was obtained from conservation conditions, and the density of channels at any point was then assumed to be proportional to the magnitude of the molar gas flux calculated at that point. This has the advantage of being relatively easy to compute, but it doesn't give one the sort of irregular random shotgun pattern of the upper termini of the channels which was observed by Leeson et al. (7) in their field study or which we observed in small-scale experiments aerating saturated sand in a large bucket. The observed irregular distribution of the channels can be expected to result in a decrease in the removal rate of VOC by sparging below that calculated from these models.

Here we present a sparging model for the removal of dissolved VOC and NAPL under conditions of mass transport-limited kinetics. The coordinates of the upper termini of the desired number of air channels are selected by means of a random number generator which produces numbers having a Gaussian distribution and a specified standard deviation. The

channel paths are then calculated as smooth curves between the point of air injection and the upper termini of the paths. Mass transport of VOC from the bulk aqueous phase to these channels is then assumed to take place by diffusion/dispersion, with irreversible removal of VOC once it reaches a channel.

The next section first presents the procedure for calculating the upper termini to the channels and the channel paths. This is followed by analysis of 1) the diffusion/dispersion transport of dissolved VOC between the various volume elements into which the system is partitioned, 2) mass transport of VOC between the aqueous phase in a volume element containing an air channel and the channel itself, and 3) the solution of NAPL droplets. This section is followed by a section on results, in which the dependence of VOC removal on the various model parameters is investigated. The paper closes with a section on conclusions and recommendations.



## ANALYSIS

### Calculation of Coordinates of Channel Upper Termini and the Channel Paths

The geometry and some of the notation used are indicated in Fig. 1, which shows the domain of interest, the point of air injection, some representative air channels, and a volume element through which one of the channels passes. This volume element is magnified in Fig. 2, in which the channel is approximated as passing vertically through the volume element and having an effective radius of $a$ meters. The nomenclature used is shown in Table 1.

The calculation of the coordinates of the upper terminus of the $m$th channel, $x_m$ and $y_m$, is done as follows. Large sets of numbers $G$ generated by the formula

$$G = 2\sqrt{\frac{3}{n'}}\sum_{i=1}^{n'}[\mathrm{RND}(1) - 0.5], \qquad n > 10 \tag{1}$$

have mean values centered on and very close to zero, standard deviations centered on and very nearly 1, skewnesses centered on and very nearly zero, and kurtoses centered on and very nearly 3. These are the values which one would expect for normal (Gaussian) distributions with $\langle G\rangle = 0$ and $\sigma_G = 1$. The distributions of these sets of numbers are bell-shaped and well-fitted by the usual Gaussian curve. In Eq. (1), RND(1) is a pseudo-random number generator which generates numbers which are

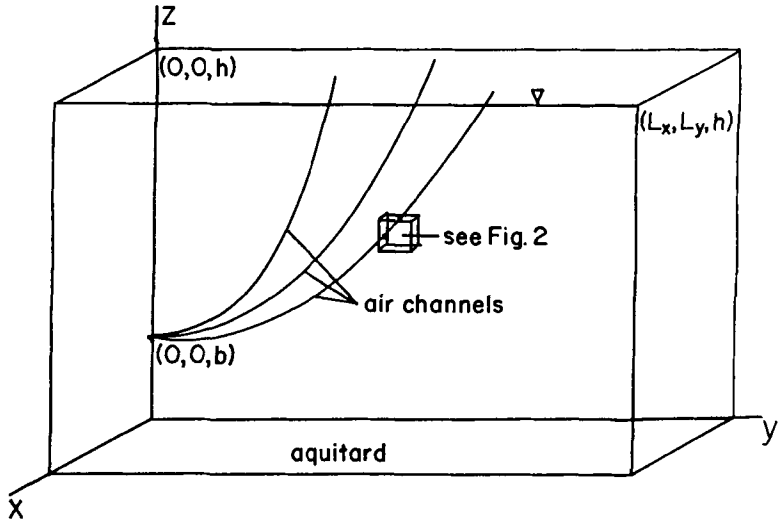


FIG. 1 Geometry and notation of that part of the domain of interest in the first quadrant. The sparging air is injected at the point $(0,0,b)$ on the $z$-axis. Three of the random air channels are shown, one of which passes through the volume element $\Delta V_{ijk}$ as indicated. The surface of the aquitard is the plane $z = 0$; the top of the aquifer is the plane $z = h$.

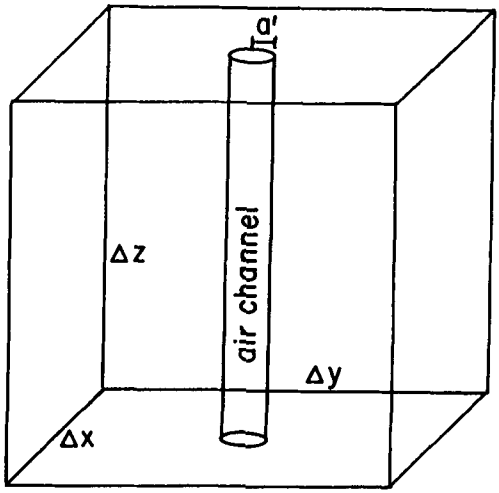


FIG. 2 Blow-up of the volume element $\Delta V_{ijk}$ indicated in Fig. 1. $a'$ = radius of air channel, $d = (\Delta x + \Delta y)/4$. VOC diffusing into the air channel is assumed to be immediately removed, so the gas-phase VOC concentration in the air channel is zero.

TABLE I
Nomenclature

| | |
|---|---|
| $h$ | thickness of aquifer, m |
| $2L_x$ | length of one side of the domain of interest, m |
| $2L_y$ | length of second side of the domain of interest, m |
| $n$ | air channel shape parameter; see Eqs. (5) and (6) |
| $\langle x \rangle$ | mean value of $x$-coordinate of air channel termini, m |
| $\langle y \rangle$ | mean value of $y$-coordinate of air channel termini, m |
| $\sigma_x$ | standard deviation of $x$-coordinate of air channel termini, m |
| $\sigma_y$ | standard deviation of $y$-coordinate of air channel termini, m |
| $b$ | height of sparging point above aquitard, m |
| $\Delta x$, $\Delta y$, $\Delta z$ | dimensions of a volume element, m |
| $D_f$ | dispersivity, $m^2/s$ |
| $D$ | VOC diffusivity in NAPL boundary layer, $m^2/s$ |
| $\nu$ | total connected porosity of aquifer medium, dimensionless |
| $2a'$ | air channel diameter, m |
| $\rho_{OC}$ | VOC density, $kg/m^3$ |
| $C_s$ | VOC solubility, $kg/m^3$ |
| $C_0$ | initial aqueous VOC concentration, $kg/m^3$ |
| $C_0^N$ | initial NAPL concentration, $kg/m^3$ of soil |
| $2a_0$ | initial NAPL droplet diameter, m |
| $b'$ | NAPL droplet boundary layer thickness, m |



uniformly distributed on (0, 1). This function is available in the various versions of BASIC, PASCAL, FORTRAN, etc.

For an experimental distribution of air channel upper termini [such as those provided by Leeson, Hinchee and Vogel (7)], one can calculate the values of $\langle x \rangle$, $\langle y \rangle$, $\sigma_x$, and $\sigma_y$. To construct a statistically similar set of termini, let the coordinates of the $m$th terminus be given by

$$z_m = h \text{ (top of the aquifer)} \tag{2}$$

$$x_m = \langle x \rangle + \sigma_x G' \tag{3}$$

$$y_m = \langle y \rangle + \sigma_y G'' \tag{4}$$

where $G'$ and $G''$ are calculated by the use of Eq. (1).

Let (0, 0, $b$) be the coordinates of the point at which the sparging air is injected. Then we may construct smooth channels between this point and the various upper termini by means of Eqs. (5) and (6).

$$x(z) = x_m \left[ \frac{z - b}{h - b} \right]^{1/n} \tag{5}$$

$$y(z) = y_m \left[\frac{z - b}{h - b}\right]^{1/n} \tag{6}$$

The parameter $n$ is a channel shape factor; $n = 1$ gives straight lines, $n = 2$ gives parabolas, etc. As $n$ becomes very large, the channel becomes L-shaped, going out horizontally from the injection point until it is underneath the upper terminus, and then rising vertically to it. Note that $x$ and $y$ are not defined for $z < b$—the channels do not go below the point of air injection.

The air channels defined in this way are smooth in character, which is in all probability somewhat unrealistic. We are developing another model in which the channels are constructed by a random-walk process; this leads to rather tortuous channels. We speculate that the two approaches to channel construction will not lead to substantial differences in calculated sparging remediation rates.



## Diffusion/Dispersion Transport between Volume Elements

For aqueous phase dispersion transport we use the usual second-order difference representation. We postulate impermeable boundary surfaces to the domain of interest with regard to dispersion transport. This is certainly valid for the bottom (aquitard) and top (water table) surfaces. If we select $\langle x \rangle$ and $\langle y \rangle = 0$ and choose a contaminant distribution which is symmetrical about the $z$-axis, it is approximately valid for the $x$–$z$ and $y$–$z$ planes, from symmetry. It will also be approximately valid at the two remaining vertical planes if the well of interest is one which is in a regular array, and $L_x$ and $L_y$ are half the distances between adjacent wells in the $x$ direction and the $y$ direction, respectively. If we are dealing with a single well, $L_x$ and $L_y$ must be selected large enough so that the boundary condition on these two surfaces is irrelevant.

With these boundary conditions, dispersion transport is modeled by Eq. (7).

$$\left[\frac{\partial C_{ijk}}{\partial t}\right]_{\text{disp}} = (D_f/v)\left\{\frac{1}{(\Delta x)^2}\left[(C_{i+1,j,k} - C_{ijk})\text{SP}(i, n_x) + (C_{i-1,j,k} - C_{ijk})\text{SM}(i)\right]\right.$$
$$+ \frac{1}{(\Delta y)^2}\left[(C_{i,j+1,k} - C_{ijk})\text{SP}(j, n_y) + (C_{i,j-1,k} - C_{ijk})\text{SM}(j)\right]$$
$$\left. + \frac{1}{(\Delta z)^2}\left[(C_{i,j,k+1} - C_{ijk})\text{SP}(k, n_z) + (C_{i,j,k-1} - C_{ijk})\text{SM}(k)\right]\right\} \tag{7}$$

where

$$\begin{aligned} \mathrm{SP}(i, n) &= 0, \quad i = n \\ &= 1, \quad i < n \end{aligned} \tag{8}$$

and

$$\begin{aligned} \mathrm{SM}(i) &= 0, \quad i = 1 \\ &= 1, \quad i > 1 \end{aligned} \tag{9}$$

SP($j$, $n$), SP($k$, $n$), SM($j$), and SM($k$) are defined in the same fashion. Equations (8) and (9), easily implemented with the SGN function, are switching functions to suppress unwanted flux terms at the boundaries of the domain of interest. Equation (7) can readily be modified to handle anisotropic dispersivities if desired.



### Diffusion/Dispersion Mass Transport to the Air Channels

See Fig. 2 for the geometry of the situation being analyzed. It is approximated that the air channel passes vertically through the volume element of interest, as indicated in the drawing. We take the diffusion of VOC in the near vicinity of this channel as governed by

$$\frac{\partial C}{\partial t} = D_f \frac{1}{r} \frac{\partial}{\partial r} \left[ r \frac{\partial C}{\partial r} \right], \qquad r > a' \tag{10}$$

We assume that the rate of replenishment of VOC in this volume element by diffusion/dispersion from adjacent volume elements matches the rate of depletion of VOC by diffusion to the air channel (the steady-state approximation). We also assume that the rate of air flow through the channel is sufficiently large to maintain a gas-phase VOC concentration far below that which would pertain if the aqueous and gas phases were to come to equilibrium. That is, we are considering only situations in which the gas flow rate is not limiting. The steady-state approximation and Eq. (10) then yield

$$\frac{1}{r} \frac{\partial}{\partial r} \left[ r \frac{\partial C}{\partial r} \right] = 0 \tag{11}$$

This equation has as its solution

$$C(r) = c_1 + c_2 \log_e(r), \qquad a < r \tag{12}$$

where $c_1$ and $c_2$ are the constants of integration.

Boundary conditions are

$$C(a') = 0 \tag{13}$$

and

$$C(d) = C_{ijk} \tag{14}$$

where $d = (\Delta x + \Delta y)/4$. Equation (13) is obtained from the assumption that the gas-phase VOC concentration in the channel is negligible. Equation (14) comes from the requirement that within the volume element of interest yet at a substantial distance $d$ from the air channel, $C(r)$ must be nearly equal to the VOC concentration $C_{ijk}$ assigned to this volume element. Use of these boundary conditions yields

$$c_2 = \frac{C_{ijk}}{\log_e(d/a')} \tag{15}$$

We wish to calculate the flux of VOC from $V_{ijk}$ into the air channel. This is given by

$$\nu\Delta x\Delta y\Delta z \left[\frac{\partial C_{ijk}}{\partial t}\right]_{\text{channel}} = -D_f 2\pi a'\Delta z \left[\frac{\partial C}{\partial r}\right]_{r=a'} \tag{16}$$

From Eqs. (12) and (15) we have

$$\left|\frac{\partial C}{\partial r}\right|_{r=a'} = \frac{C_{ijk}}{\log_e(d/a')}\frac{1}{a} \tag{17}$$

This, with Eq. (16), gives

$$\left[\frac{\partial C_{ijk}}{\partial t}\right]_{\text{channel}} = -\frac{2\pi D_f C_{ijk}}{\nu\Delta x\Delta y \log_e(d/a')} \tag{18}$$

## Kinetics of the Solution of NAPL Droplets

For analyzing the solution of NAPL droplets we use an approach used previously for the solution of NAPL in groundwater recovery operations (18) and sparging (19). We assume spherical droplets and a fixed outer radius $b$ of the diffusion boundary layer surrounding each droplet. Notation in this section only is as follows.

$\rho_{OC}$ = density of NAPL VOC, kg/m$^3$
$\Delta V = \Delta x\Delta y\Delta z$, the volume of a volume element, m$^3$
$a_0$ = initial droplet radius, m
$a$ = droplet radius at time $t$, m
$n$ = number of droplets in $\Delta V$

$C_0^N$ = initial NAPL concentration in $\Delta V$, kg/m$^3$ of soil
$C^N$ = NAPL concentration in $\Delta V$ at time $t$, kg/m$^3$ of soil
$m_0$ = initial droplet mass, kg
$m$ = droplet mass at time $t$, kg
$C_s$ = aqueous solubility of VOC, kg/m$^3$ of water
$C_{ikj}$ = aqueous VOC concentration in the $ijk$th volume element, kg/m$^3$ of water

We have

$$n \frac{4\pi a_0^3 \rho_{OC}}{3} = \Delta V C_0^N \tag{19}$$

from which we see that the number of droplets in the volume element of interest is

$$n = \frac{3\Delta V C_0^N}{4\pi a_0^3 \rho_{OC}} \tag{20}$$

We assume steady-state diffusion in the vicinity of a droplet, which yields

$$\frac{1}{r^2} \frac{\partial}{\partial r} \left[ r^2 \frac{\partial C(r)}{\partial r} \right] = 0 \tag{21}$$

which has as its solution

$$C(r) = c_1/r + c_2 \tag{22}$$

where $c_1$ and $c_2$ are the constants of integration. The boundary conditions are

$$C(a) = C_s \tag{23}$$

and

$$C(b) = C_{ijk} \tag{24}$$

Use of Eqs. (23) and (24) in Eq. (22) gives

$$c_1 = (C_s - C_{ijk})ab/(b - a) \tag{25}$$

Substitution of this result in Eq. (22) and differentiation yields

$$\frac{C(r)}{r} = -\frac{(C_s - C_{ijk})ab}{(b - a)r^2} \tag{26}$$

Evaluation of Eq. (26) at $r = a$ gives

$$\left.\frac{\partial C(r)}{\partial r}\right|_{r=a} = -\frac{(C_s - C_{ijk})ab}{(b - a)a^2} \tag{27}$$

The rate of change of mass $m$ of a droplet is then given by

$$\frac{dm}{dt} = D(4\pi a^2)\left[-\frac{C_s - C_{ijk}}{(b - a)a^2}\, ab\right] \tag{28}$$

$$\frac{dm}{dt} = -4\pi D(C_s - C_{ijk})\frac{ba}{(b - a)} \tag{29}$$

Note that

$$m = \Delta V C^N/n \tag{30}$$

$$m_0 = \Delta V C_0^N/n \tag{31}$$

and

$$a = \left[\frac{3m}{4\pi\rho_{OC}}\right]^{1/3} \tag{32}$$

$$a_0 = \left[\frac{3m_0}{4\pi\rho_{OC}}\right]^{1/3} \tag{33}$$

Use of these relationships in Eq. (29) and some algebraic simplification then yield

$$\frac{dC_{ijk}^N}{dt} = -\frac{3DC_0^N}{a_0^2\rho_{OC}}\frac{(C_s - C_{ijk})(C_{ijk}^N/C_0^N)^{1/3}}{[1 - (a_0/b)(C_{ijk}^N/C_0^N)^{1/3}]} \tag{34}$$

where we have now subscripted $C^N$ ($=C_{ijk}^N$) to indicate the volume element involved.

The contribution of NAPL solution to the rate of change of the aqueous VOC concentration, $C_{ijk}$, is given by

$$\left[\frac{\partial C_{ijk}}{\partial t}\right]_{\text{solution}} = -(1/v)\frac{dC_{ijk}^N}{dt} \tag{35}$$

## The Rate of Change of the Aqueous VOC Concentration. Residual VOC

The total rate of change of the aqueous VOC concentration is then given by the sum of its contributions from solution of NAPL, diffusion/

dispersion between volume elements, and diffusion/dispersion to the air channels,

$$\frac{dC_{ijk}}{dt} = \left[\frac{\partial C_{ijk}}{\partial t}\right]_{\text{solution}} + \left[\frac{\partial C_{ijk}}{\partial t}\right]_{\text{disp}} + \left[\frac{\partial C_{ijk}}{\partial t}\right]_{\text{channel}} \tag{36}$$

where the components on the right-hand side of Eq. (36) are given by Eqs. (35), (18), and (7), respectively.

Residual VOC present as NAPL and dissolved VOC at time $t$ are given by

$$M_{\text{NAPL}}(t) = \Delta V \sum_{i=1}^{n_x} \sum_{j=1}^{n_y} \sum_{k=1}^{n_z} C_{ijk}^{\text{N}} \tag{37}$$

and

$$M_{\text{aq}}(t) = \nu \Delta V \sum_{i=1}^{n_x} \sum_{j=1}^{n_y} \sum_{k=1}^{n_z} C_{ijk} \tag{38}$$

respectively.

## RESULTS

The model was implemented in TurboBASIC; the differential equations were integrated forward in time by means of the simple Euler method,

TABLE 2
Default Parameters for Sparging Simulations, Dissolved VOC Only

| | |
|---|---|
| Channel shape parameter $n$ | 4 |
| $0 < x < L_x$; $L_x$ | 10 m |
| $0 < y < L_y$; $L_y$ | 10 m |
| Thickness of aquifer, $h$ | 10 m |
| Number of channels in first octant | 50 |
| $\langle x \rangle$, $\langle y \rangle$ | 0 |
| $\sigma_x$, $\sigma_y$ | 4 m |
| Height of sparging point above aquitard, $b$ | 0 |
| $\Delta x$, $\Delta y$ | 1 m |
| $\Delta z$ | 1 m |
| Dispersivity, $D_f$ | $2.0 \times 10^{-7}$ m$^2$/s |
| Porosity, $\nu$ | 0.4 |
| Air channel diameter, $2a'$ | 1 cm |
| $\Delta t$ | 43,200 seconds |
| Initial aqueous VOC concentration | 10 mg/L |
| Entire domain of interest uniformly contaminated with dissolved VOC only | |

since computer memory and speed limitations made use of any more sophisticated algorithm impractical. Default parameters for the runs made with dissolved VOC only are given in Table 2. Default parameters for the runs made with NAPL and dissolved VOC are given in Table 3. Densities and aqueous solubilities of VOCs which were simulated are given in Table 4.

Figure 3 shows a representative set of air channels in profile view. Only one-fourth of the domain of interest is modeled; air is assumed to be injected at the origin, and we are considering only channels in the first quadrant. Figure 4 is a plan view of the same system, showing the locations of the terminations of the air channels at the top of the aquifer. The $x$ and $y$ scales are different, owing to the vagaries of EGA monitors. The parameters are as in Table 2.

Even when all the parameters of the model are held fixed, one obtains somewhat different removal rates depending on the set of random numbers which are generated and which determine the paths followed by the air channels. The magnitude of this effect is shown in Fig. 5, in which five runs which are identical in all respects except for the seeding of the random



TABLE 3
Default Parameters for Sparging Simulations, Dissolved VOC and NAPL

| | |
|---|---|
| Channel shape parameter $n$ | 4 |
| $0 < x < L_x$; $L_x$ | 10 m |
| $0 < y < L_y$; $L_y$ | 10 m |
| Thickness of aquifer, $h$ | 10 m |
| Number of channels in first octant | 50 |
| $\langle x \rangle$, $\langle y \rangle$ | 0 |
| $\sigma_x$, $\sigma_y$ | 6 m |
| Height of sparging point above aquitard, $b$ | 0 |
| $\Delta x$, $\Delta y$ | 1 m |
| $\Delta z$ | 1 m |
| Dispersivity, $D_f$ | $2.0 \times 10^{-7}$ m$^2$/s |
| VOC diffusivity in NAPL boundary layer, $D$ | $2.0 \times 10^{-10}$ m$^2$/s |
| Porosity, $\nu$ | 0.4 |
| Air channel diameter, $2a'$ | 1 cm |
| $\Delta t$ | 17,280 seconds |
| VOC density, $\rho_{OC}$ | 1.46 g/cm$^3$ |
| VOC solubility, $C_s$ | 1100 mg/L |
| Initial aqueous VOC concentration, $C_0$ | 100 mg/L |
| Initial NAPL concentration $C_0^N$ | 1000 mg/kg of soil |
| Initial NAPL droplet diameter, $2a_0$ | 1 mm |
| Droplet boundary layer thickness, $b$ | 500 mm |

TABLE 4
Densities and Aqueous Solubilities of VOCs (estimated from data in Ref. 20)

| Compound | Density (g/cm$^3$) | Aqueous solubility, 20°C (mg/L) |
|---|---|---|
| *n*-Octane | 0.7025 | 0.431 |
| Benzene | 0.877 | 1800 |
| Toluene | 0.867 | 520 |
| Ethylbenzene | 0.867 | 152 |
| Xylenes | 0.870 | 160 |
| Trichloroethylene | 1.46 | 1100 |
| Tetrachloroethylene | 1.623 | 150 |
| 1,1,1-Trichloroethane | 1.339 | 600 |
| 1,1-Dichloroethylene | 1.22 | 2500 |
| *trans*-1,2-Dichloroethylene | 1.257 | 6300 |
| Carbon tetrachloride | 1.593 | 800 |
| 1,1,2,2-Tetrachloroethane | 1.595 | 2900 |



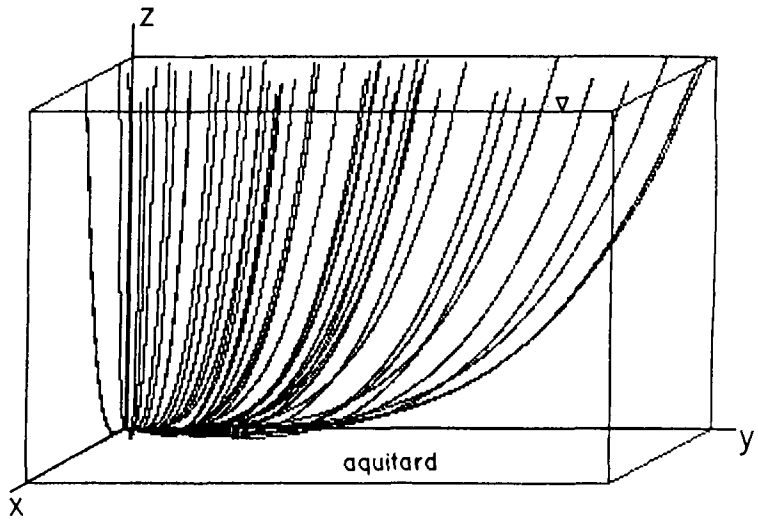


FIG. 3 Locations of air channel termini at the top of the aquifer. $\langle x \rangle = \langle y \rangle = 0$; $\sigma_x = \sigma_y = 4$ m; $L_x = L_y = h = 10$ m, 50 channels calculated. Note that the origin is in the upper left corner of the figure, and that the $x$ and $y$ scales are different. Figure 4 shows plots of the air channels associated with these termini.

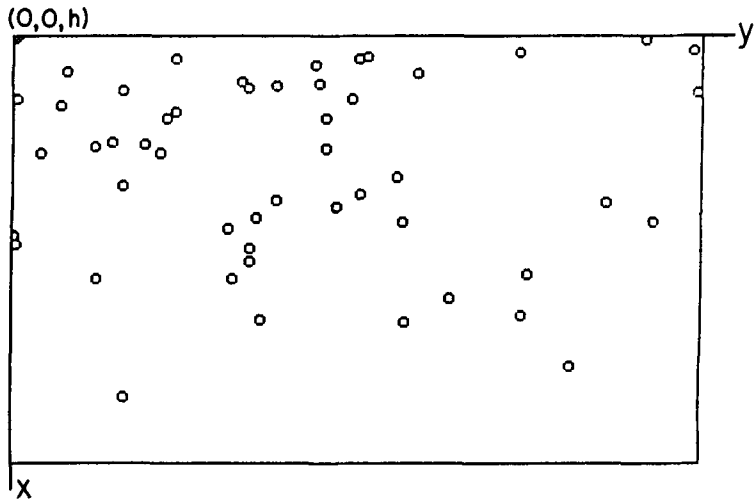


FIG. 4 Plots of air channels in the domain of interest. The parameters are as in Fig. 3; $n = 4$. Note that the $x$, $y$, and $z$ scales are different.

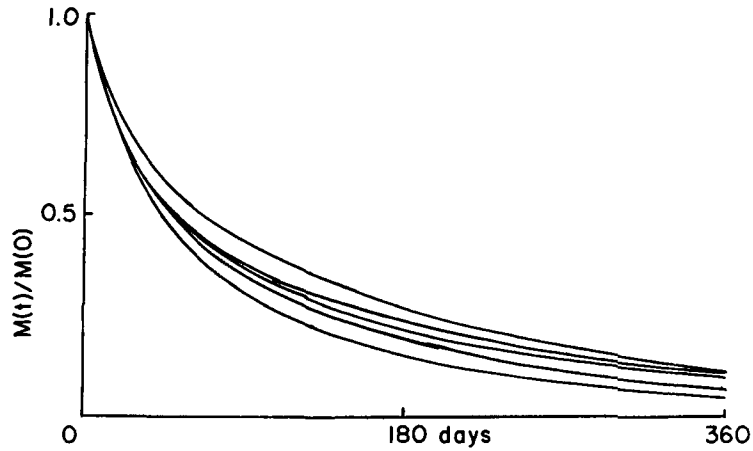


FIG. 5 Plot of $M_{aq}(t)/M_{aq}(0)$ versus $t$, only dissolved VOC present; reproducibility of statistically equivalent runs. $\sigma_x = \sigma_y = 5$ m; other parameters as in Table 2. These runs are statistically equivalent; the variations between them are due to the random variations between the different sets of air channel paths.

number generator RND are plotted. The uncertainty seen here represents an intrinsic limit on channeling models unless one is prepared to map out in detail the channels for each and every sparging well at a site—a task of awesome proportions. Only dissolved VOC is present in the runs shown in Figs. 5–11.

The effect of the effective radius of the air channel distribution on dissolved VOC removal is seen in Fig. 6. The standard deviations of the channel termini about (0, 0, $h$) are $\sigma_x = \sigma_y = 4$, 5, and 6 m. The effective radii of the gas distributions for the three runs are about 1.414 times these values. We see that the removal rate increases with increasing effective radius of the gas distribution. This is expected, since the distributions having the smaller effective radii leave substantial portions of the outer and lower portions of the domain of interest without air channels. In the runs shown in Figs. 6 through 14, the random number generator was seeded with a constant value (13) to avoid the confounding effects of these random statistical variations.

Increasing the number of air channels increases the rate of dissolved contaminant removal, as expected and as shown in Fig. 7. Increasing the number of air channels decreases the average distance VOC must move



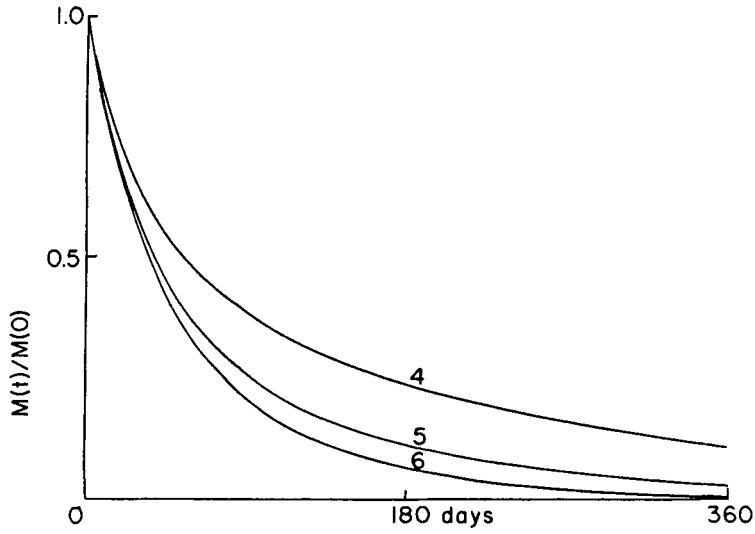


FIG. 6 Plot of $M_{aq}(t)/M_{aq}(0)$ versus $t$, only dissolved VOC present; effect of $\sigma_x$ and $\sigma_y$. $\sigma_x = \sigma_y = 4$, 5, and 6 m, as indicated. Other parameters as in Table 2. RND seeded with the same number for all runs.

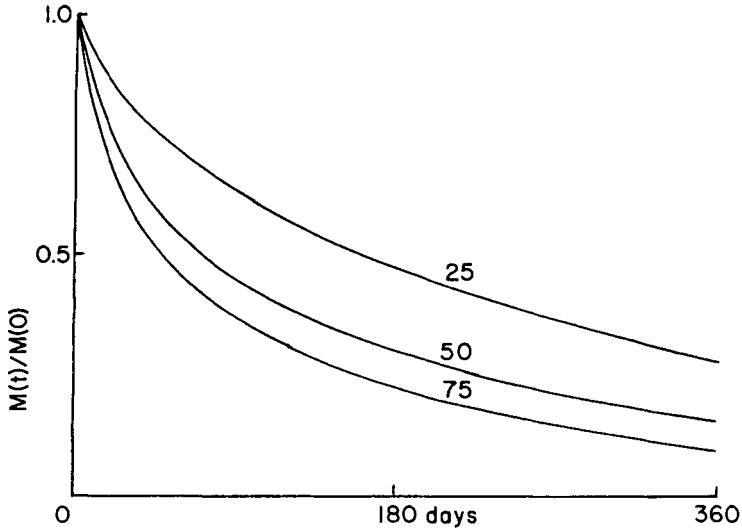


FIG. 7 Plot of $M_{aq}(t)/M_{aq}(0)$ versus $t$, only dissolved VOC present; effect of number of channels. $\sigma_x = \sigma_y = 6$ m; 25, 50, and 75 channels, as indicated. Other parameters as in Table 2. RND seeded with the same number for all runs.



by dispersion before it can reach an air channel and be removed. Unfortunately, at sites at which the water table lies below grade (virtually all sites), there appears to be no way by which one can estimate the number of air channels and how this quantity depends on well depth and the pressure of the injected air. One can use the results reported by Leeson et al. (7), but one would prefer to have a method for obtaining site-specific information on this.

The shapes of the channels (controlled by the parameter $n$ in Eqs. 5 and 6) have a very marked effect on the efficiency of dissolved VOC removal, as seen in Fig. 8. Examination of these equations shows that the channels tend to pass through more of the low-lying volume elements of the domain of interest as $n$ increases. Values of $n$ of 1 and 0.5 yield channel distributions which completely miss a substantial portion of the lower and outer portions of the domain. This is reflected in correspondingly slow removal rates.

The effect of the dispersivity $D_f$ on dissolved VOC removal is seen in Fig. 9. Cleanup times appear to be roughly inversely proportional to $D_f$, indicating that dispersive transport of dissolved VOC to the air channels is rate limiting, expected in this model. Evidently, anything which can be

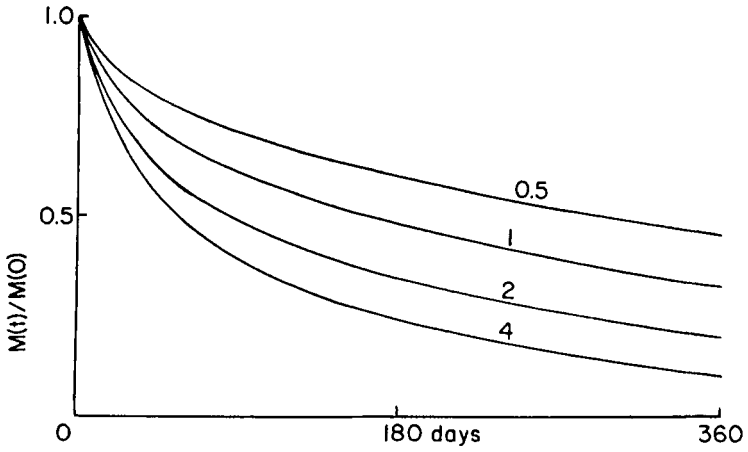


FIG. 8 Plot of $M_{aq}(t)/M_{aq}(0)$ versus $t$, only dissolved VOC present; effect of air channel shape parameter $n$. $n$ = 0.5, 1, 2, and 4 as indicated; other parameters as in Table 2. RND seeded with the same number for all runs.



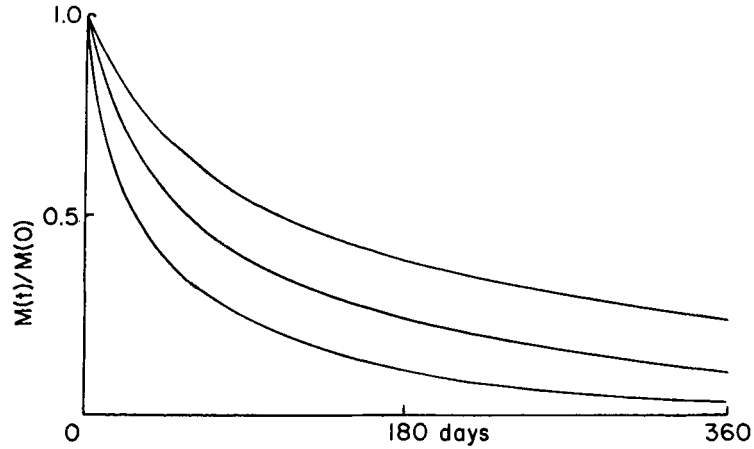


FIG. 9 Plot of $M_{aq}(t)/M_{aq}(0)$ versus $t$, only dissolved VOC present; effect of diffusivity. $D_f$ = 1, 2, and 4 $\times$ $10^{-7}$ $m^2/s$ from top to bottom; other parameters as in Table 2. RND seeded with the same number for all runs.

done to increase the dispersivity (such as pulsed operation of the air injection well) will result in increased rate of VOC removal.

In the runs shown in Figs. 5–9 and 11–14, the dimensions of the domain of interest are 10 × 10 × 10 m—i.e., the wells are drilled in a square array 20 m apart and the aquifer is 10 m thick. In Fig. 10 the domain dimensions are 20 × 20 × 10, 15 × 15 × 10, and 10 × 10 × 10, corresponding to sparging well spacings of 40, 30, and 20 m on a square grid. All other parameters are held constant. In particular, the dimensions of the initially contaminated domain are held constant. As the spacing of the wells increases, we see progressively more and more severe tailing in the remediation. Dispersion is transporting dissolved VOC to the more outlying portions of the domain which contain few if any air channels. Once VOC has migrated into these, its movement back into the region of active aeration (i.e., significant density of channels) is slow, resulting in this tailing. If one were sparging with wells located only in the zone of contamination and without plume control by groundwater recovery wells, this could also result in the spreading of contaminant beyond the effective range of capture of the sparging wells. Evidently sparging wells operating in the contaminated zone should be surrounded by a border of sparging wells just beyond the periphery of the contaminated zone to prevent escape of contaminant into the surrounding aquifer.



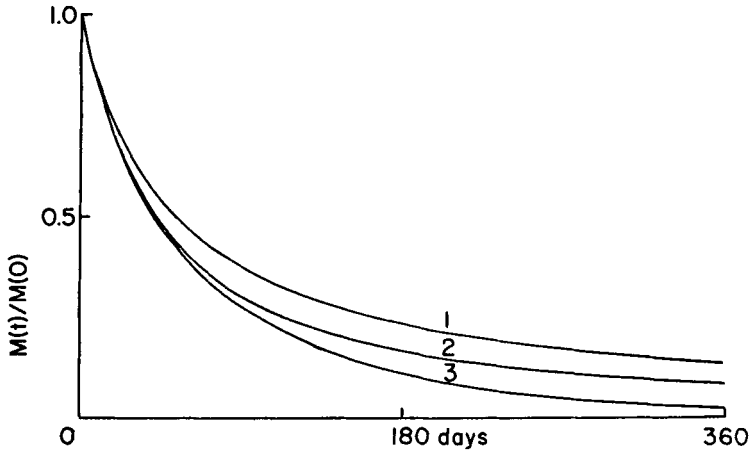


FIG. 10 Plot of $M_{aq}(t)/M_{aq}(0)$ versus $t$, only dissolved VOC present; effect of size of domain of interest. From top to bottom, $(L_x, L_y, h)$ = [1] (20, 20, 10); [2] (15, 15, 10), [3] (10, 10, 10). The initial domain of contamination is included in the ranges $0 < x < 10$; $0 < y < 10$; $3 < z < 10$ m in all cases. $\sigma_x = \sigma_y = 6$ m. Other parameters as in Table 2. RND seeded with the same number for all runs.

The impact of the depth of the point of air injection on dissolved VOC removal is shown in Fig. 11. It is evident that sparging wells must be drilled entirely through the domain of contamination in order to be optimally effective. Shallow sparging wells leave virtually untreated that portion of the aquifer which lies below the point of air injection.

Figures 12–14 address the removal of distributed NAPL; default parameters for these runs are given in Table 3. In Fig. 12 the effect of the diffusivity in the aqueous boundary layers surrounding the NAPL droplets is shown. The VOC simulated here is trichloroethylene and the dispersivity is assumed to be $2 \times 10^{-7}$ m$^2$/s. For this system, diffusion of VOC through the aqueous boundary layers around the NAPL droplets becomes the limiting factor in VOC removal only for values of the diffusivity below around $1\text{–}2 \times 10^{-11}$ m$^2$/s. Typical values of molecular diffusion constants in water are of the order of $2 \times 10^{-10}$ m$^2$/s. We conclude that in many systems bulk dispersivity of dissolved VOC is more likely to be rate controlling than is diffusion-limited solution of NAPL.

Figure 13 shows the results of modeling the removals of some volatile hydrocarbons (*n*-octane, benzene, toluene, ethylbenzene, and xylenes) initially present as NAPL. The solubilities and densities of these com-



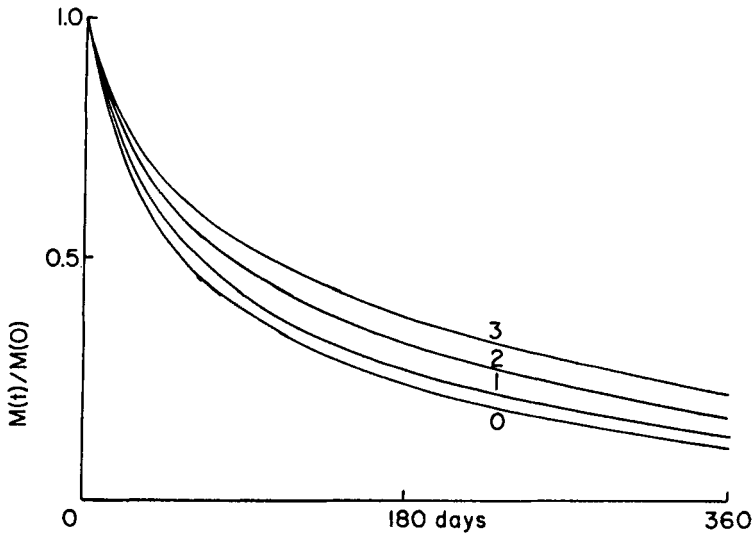


FIG. 11 Plot of $M_{aq}(t)/M_{aq}(0)$ versus $t$, only dissolved VOC present; effect of height $b$ of air injection point above the underlying aquitard. $b$ = 3, 2, 1, and 0 m, from top to bottom. Other parameters as in Table 2. RND seeded with the same number for all runs.

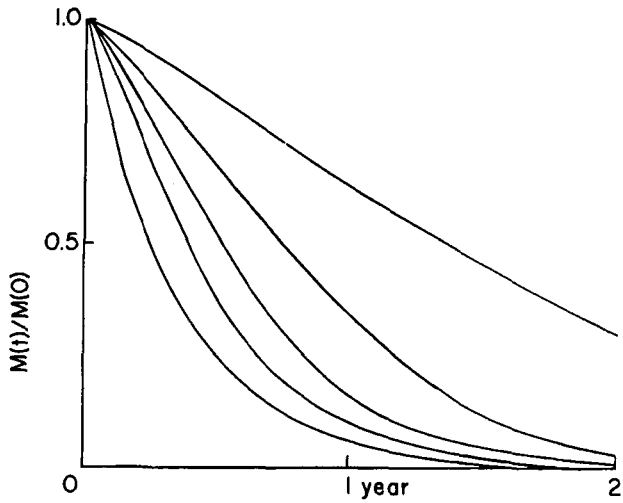


FIG. 12 Plot of $M_{aq}(t)/M_{aq}(0)$ versus $t$, NAPL and dissolved VOC present; effect of diffusivity $D$ in NAPL droplet boundary layers. $D = 2 \times 10^{-12}$, $5 \times 10^{-12}$, $1 \times 10^{-11}$, $2 \times 10^{-11}$, and $2 \times 10^{-9}$ m$^2$/s, from the top down; other parameters as in Table 3. RND seeded with the same number for all runs.

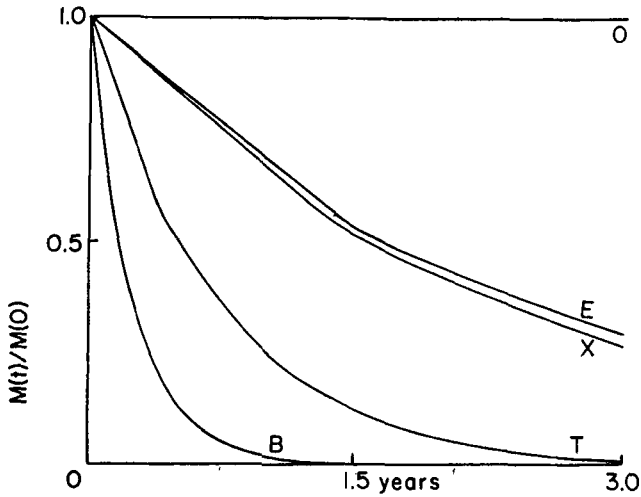


FIG. 13 Plot of $M_{aq}(t)/M_{aq}(0)$ versus $t$ for $n$-octane (O), benzene (B), toluene (T), ethylbenzene (E), and xylene (X) compounds; LNAPL and dissolved VOC present. VOC solubilities and LNAPL densities are given in Table 4. The initial dissolved VOC concentrations are 0.1 times the corresponding solubilities; the initial LNAPL concentrations are all 1000 mg/kg of soil. Other parameters as given in Table 3.

pounds are given in Table 4; other parameters are as in Table 3. In all cases the initial NAPL concentration is 1000 mg/kg of soil. Benzene and toluene are readily removed within 3 years; xylenes and ethylbenzene are somewhat less rapidly removed. Removal of the alkane *n*-octane is negligible during the 3-year span of the simulations. The reason for the spectacular difference is seen in Eq. (34). The rate of removal of VOC is controlled here by the rates of solution of the NAPL droplets and dispersion of the dissolved VOC. These are essentially proportional to the aqueous solubility of the VOC. The solubilities of toluene and *n*-octane are 520 and 0.431 mg/L, respectively, which accounts for the great difference in the removal rates of the two compounds.

With compounds of low aqueous solubility, such as *n*-octane, it is impossible to maintain concentration gradients large enough to cause solution of NAPL and dispersion of dissolved VOC to take place at a reasonable rate. This appears to explain why the BTEX group is removed relatively rapidly by sparging, while total petroleum hydrocarbons (which includes a lot of alkanes of low aqueous solubility) are sparged much less readily. One possible solution to the dilemma is to dewater smear zones so that these compounds must move through only very thin layers of water in order to vaporize, and use soil vapor extraction.



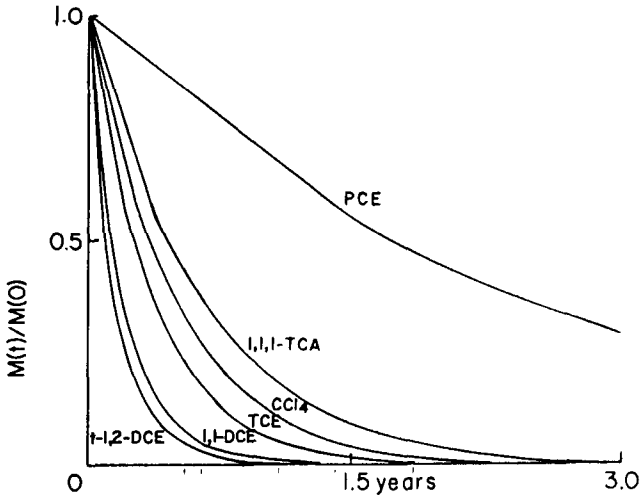


FIG. 14 Plot of $M_{aq}(t)/M_{aq}(0)$ versus $t$ for several chlorinated solvents; DNAPL and dissolved VOC present. Chlorinated VOC solubilities and DNAPL densities are given in Table 4. The initial dissolved VOC concentrations are 0.1 times the corresponding solubilities; the initial DNAPL concentrations are all 1000 mg/kg of soil. Other parameters as given in Table 3.

TABLE 5
95 and 99% Cleanup Times for Various VOCs Initially Present at NAPL Concentrations of 1000 mg/kg of Soil

| Compound | 95% Cleanup time (years) | 99% Cleanup time (years) |
|---|---|---|
| *n*-Octane | ∞ | ∞ |
| Benzene | 0.7 | 1.2 |
| Toluene | 2.1 | 3.0 |
| Ethylbenzene | 7.0 (est.) | 11 (est.) |
| Xylenes | 6.6 (est.) | 11 (est.) |
| Trichloroethylene | 1.1 | 1.8 |
| Tetrachloroethylene | 7.2 (est.) | 12 (est.) |
| 1,1,1-Trichloroethane | 1.8 | 2.7 |
| 1,1-Dichloroethylene | 0.6 | 1.2 |
| *trans*-1,2-Dichloroethylene | 0.5 | 0.85 |
| Carbon tetrachloride | 1.4 | 2.2 |
| 1,1,2,2-Tetrachloroethane | 1.4 | 2.2 |



The removals of several chlorinated solvents present as distributed DNAPL are shown in Fig. 14. Parameters are as in Tables 2 and 3. Tetrachloroethylene (PCE), the compound of lowest aqueous solubility, is the most slowly removed of the set. Note that these results definitely do not pertain to DNAPL which is pooled on the underlying aquitard, removal of which is at best extremely difficult and generally is regarded as impossible.

The times required for 95 and 99% removal of VOC for these hydrocarbons and chlorinated solvents (calculated for the runs shown in Figs. 13 and 14 and a run for 1,1,2,2-TCA which is not shown) are listed in Table 5. These results depend upon the selection of parameters for the model, particularly the dispersivity. The choice of a value for the dispersivity is open to considerable debate. The cleanup times should therefore not be interpreted too literally, but the trends and the orders of magnitude should be correct. We see again the strong correlation between removal rate and aqueous solubility. This, of course, is ultimately limited as the Henry's constant of the VOC (essentially its vapor pressure divided by its solubility) becomes sufficiently small that the rate of gas flow becomes the limiting factor. At this point our model is no longer applicable.

## CONCLUSIONS

The following conclusions can be drawn from these modeling exercises. First, however, we note again that this model is limited to situations in

which the air flow rate is sufficient that it is not the limiting factor controlling the VOC removal rate. Cleanup times calculated by this model are therefore lower bounds to those which would be expected in actuality.

- Enhancement of dispersivity by, for instance, pulsed air injection, should in most cases result in substantial improvement in the performance of air sparging systems.
- One can expect some spreading of dissolved VOC by sparging. This has been recognized by sparging practitioners for some time, and can be controlled by groundwater recovery operations and/or by the establishment of a barrier of sparging wells to intercept the spreading contaminants.
- VOCs of very low aqueous solubility (such as alkanes) will generally be removed quite slowly by sparging. A more effective alternative for removing total petroleum hydrocarbons from smear zones may be depression of the water table by groundwater recovery combined with soil vapor extraction.
- The distribution and number of air channels around a sparging well very markedly affect its efficiency. Unfortunately, at present these cannot be measured in most cases. Research on this (such as described in Ref. 7) is very much needed.
- By and large, the conclusions drawn from our earlier channeling model for sparging (effect of dispersivity, effect of sparging well depth, VOC concentration rebound after well shutdown, etc.—see Ref. 14) remain valid within the framework of the present model.



## REFERENCES

1. R. A. Brown, "Sparging: A New Technology for the Remediation of Aquifers Contaminated with Volatile Organic Compounds," in *Modeling of In Situ Techniques for Treatment of Contaminated Soils: Soil Vapor Extraction, Sparging, and Bioventing* (D. J. Wilson, Ed.), Technomic Publishing Co., Lancaster, PA, 1995.
2. M. E. Loden, *A Technology Assessment of Soil Vapor Extraction and Air Sparging*, US EPA Report EPA/600/R-92/173, Risk Reduction Engineering Laboratory, Office of Research and Development, US EPA, Cincinnati, OH, 1992.
3. W. C. Anderson (Ed.), *Innovative Site Remediation Technology: Bioremediation*, American Academy of Environmental Engineers, Annapolis, MD, 1995.
4. W. C. Anderson (Ed.), *Innovative Site Remediation Technology: Vacuum Vapor Extraction*, American Academy of Environmental Engineers, Annapolis, MD, 1995.
5. R. E. Hinchee (Ed.), *Air Sparging for Site Remediation*, Batelle Press, Columbus, OH, 1993.
6. R. E. Hinchee, R. N. Miller, and P. C. Johnson, *In Situ Aeration: Air Sparging, Bioventing, and Related Remediation Processes*, Batelle Press, Columbus, OH, 1995.
7. A. Leeson, R. E. Hinchee, and C. M. Vogel, *Evaluation of the Effectiveness of Air*

*Sparging*, Presented at In Situ and On-Site Bioreclamation: The Third International Symposium, April 24–27, 1995, San Diego, CA.
8. M. A. Dahmani, D. P. Ahlfeld, G. E. Hoag, and W. Ji, *Field Behavior of Air Sparging: Implications of a Conceptual Model*, Presented at In Situ and On-Site Bioreclamation: The Third International Symposium, April 24–27, 1995, San Diego, CA.
9. D. H. Mohr, *Mass Transfer Concepts Applied to In Situ Air Sparging*, Presented at In Situ and On-Site Bioreclamation: The Third International Symposium, April 24–27, 1995, San Diego, CA.
10. R. L. Johnson, N. R. Thomson, and P. C. Johnson, *Does Sustained Groundwater Circulation Occur during In Situ Air Sparging*, Presented at In Situ and On-Site Bioreclamation: The Third International Symposium, April 24–27, 1995, San Diego, CA.
11. F. C. Payne, A. R. Blaske, G. A. vanHouten, and J. B. Lisiecki, *Comparison of Contamination Removal Rates in Pulsed and Steady-Flow Aquifer Sparging*, Presented at In Situ and On-Site Bioreclamation: The Third International Symposium, April 24–27, 1995, San Diego, CA.
12. D. J. Wilson, C. Gomez-Lahoz, and J. M. Rodriguez-Maroto, "Groundwater Cleanup by In-Situ Sparging. VIII. Effect of Air Channeling on Dissolved Volatile Organic Compounds Removal Efficiency," *Sep. Sci. Technol.*, *29*, 2387 (1994).
13. D. J. Wilson, R. D. Norris, and A. N. Clarke, "Groundwater Cleanup by In-Situ Sparging. IX. Air Channeling Model for Nonaqueous Phase Liquid Removal," *Ibid.*, *31*, 915 (1996).
14. D. J. Wilson, R. D. Norris, and A. N. Clarke, "Groundwater Cleanup by In-Situ Sparging. X. Air Channeling Model for Biosparging of Nonaqueous Phase Liquid," *Ibid.*, *31*, 1357 (1996).
15. B. Herrling, J. Stamm, E. J. Alesi, and P. Brinnel, "Vacuum-Vaporizer-Wells (UVB) for In Situ Remediation of Volatile and Strippable Contaminants in the Unsaturated and Saturated Zones," in *Proceedings of the Symposium on Soil Venting*, April 29–May 1, 1991, Houston, TX, p. 203.
16. US EPA, *Unterdruck-Verdampfer-Brunnen Technology (UVB) Vacuum Vaporizing Well*, US EPA Site Technology Capsule, EPA/540/R-95/500a, July 1995.
17. D. J. Wilson, S. Kayano, R. D. Mutch Jr., and A. N. Clarke, "Groundwater Cleanup by In Situ Sparging. I. Mathematical Modeling," *Sep. Sci. Technol.*, *27*, 1023 (1992).
18. C. Gomez-Lahoz, R. A. Garcia-Delgado, and D. J. Wilson, "A Model with Mass Transport Limitations for Pump and Treat Remediation of Soils Polluted with NAPL," *Environ. Monitor. Assess.*, *32*, 161 (1994).
19. D. J. Wilson, "Groundwater Cleanup by In-Situ Sparging. V. Mass Transport-Limited Dense Nonaqueous Phase Liquid and Volatile Organic Compound Removal," *Sep. Sci. Technol.*, *29*, 71 (1994).
20. J. H. Montgomery and L. M. Welkom, *Groundwater Chemicals Desk Reference*, Lewis Publishers, Chelsea, MI, 1990.

*Received by editor July 3, 1996*
*Revision received April 1997*